A Method for Terrain Positioning of an AUV

Ingemar Nygren

Swedish Defence Research Agency
172 90 Stockholm, Sweden
Ingemar.Nygren@foi.se

Abstract In many autonomous underwater vehicle (AUV) applications, there is a need to accurately determine the AUV's position in an effective way in terms of both cost and energy consumption.

This paper describes a method to solve above problem. The method is conceptually simple and involves measuring the bottom topography with a few sonar pings over a limited area by an ordinary bathymetric multibeam sonar.

Navigation, according to the above method, means that the AUV with the help of the conventional navigational aids moves between navigation areas for which bottom maps are available. When the AUV is within such a navigation area its position is determined by measuring the bottom topography and then correlating it with the underwater map.

The paper deals with the positioning problem by an elementary introductory theoretical discussion and then presents some results from a simulation study with the Reson SeaBat 9001 multibeam bathymetric sonar. It also presents the results of a verification sea trial in a flat-bottom area using the same sonar.

1. Introduction

In many AUV applications, there is a need to accurately determine the AUV's position in relation to the underlying bottom structures or in relation to the coordinates on a map in an effective way, both in terms of cost and in terms of energy consumption since in most cases, the AUV is battery-powered.

A solution to the positioning problem that is often proposed is to use a method similar to the terrain navigation method, which has been used with cruise missiles. In the AUV case, a sonar will be used for continuously measuring the distance to the bottom, together with an inexpensive inertial navigation system (INS). The measurements are integrated by a Kalman filter (ref. [1]).

However, the method is not particularly accurate or energy-effective since the sonar has to work continuously. Furthermore, an underwater map has to be available of the whole area over which the AUV moves. Another problem is that the Kalman filter easily diverges.

To improve the accuracy and reduce the risk of diverges, many different variants of the Kalman filter have been tested through the years, especially for non-linear systems. A popular method, which handles the problem of non-linearity, has recently been to represent the probability distributions for the state variables by samples from these distributions and after each step in the filter algorithm, resample the distribution (ref. [2]).

This paper describes a different method of solving above problem.

2. The positioning method

The proposed method is conceptually very simple and involves measuring the bottom topography by a few sonar pings, say, five pings, over a limited area by an ordinary bathymetric multibeam sonar.

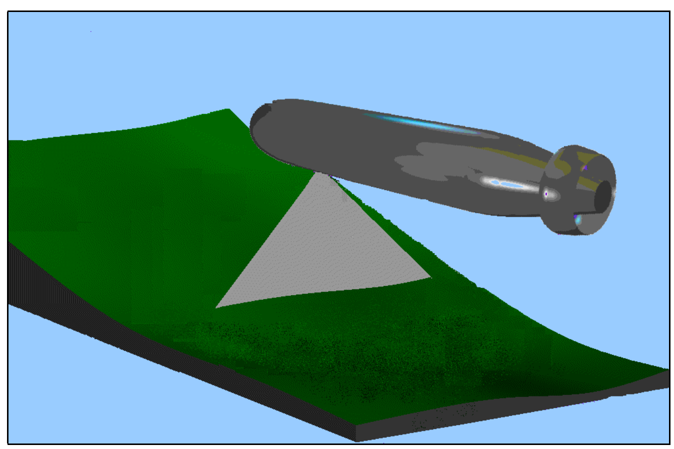

Figure 2.1. Representation of an AUV measuring the bottom topography.

The measured area, which typically has the size of 40 m x 40 m to 300 m x 300 m, depending on the height above the bottom and the sonar, is then correlated against the bottom map. The correlation is only done for areas that have the correct depth. This considerably reduces the computing burden.

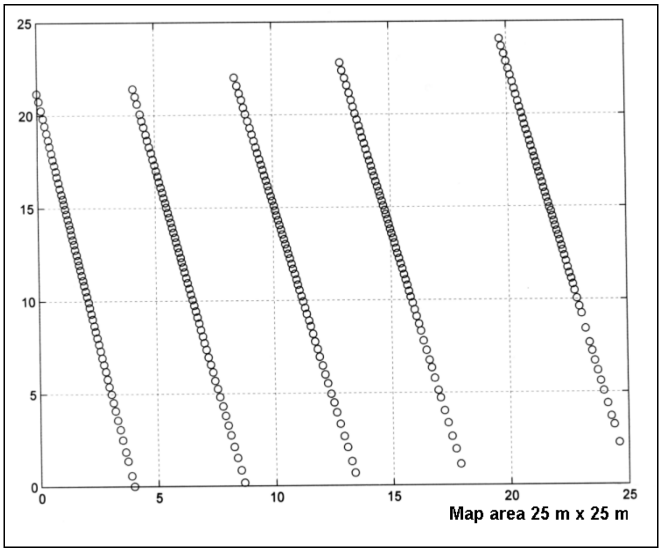

Figure 2.2. The footprint of the individual beams in five beam planes.

Navigation, according to the method, means that with the help of conventional navigation aids such as INSs, and dead reckon/Doppler-log, etc, the AUV moves between so-called **"**navigation cells**"** for which bottom maps are available (ref. [3]). When according to the AUV's measurements**,** it is within the navigation cell it determines its position by measuring the bottom topography**,** as mentioned above**,** and then correlates it with the bottom map.

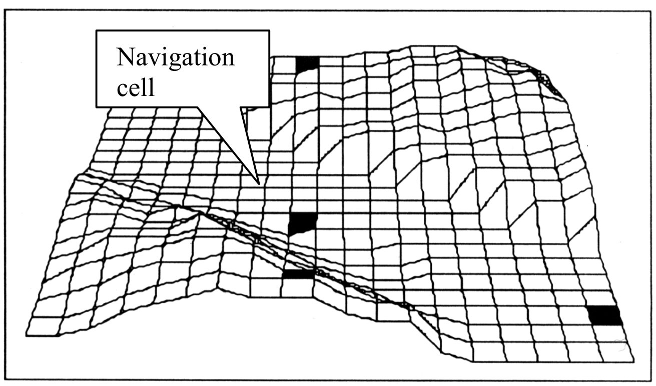

Figure 2.3. Navigation cells having good terrain correlation properties on the bottom map.

The size of the navigation cell is determined by the uncertainty of the navigation system used when traveling between the navigation cells. The size of the navigation cell has to be such that the AUV will always end up within the cell for the next determination of its position.

2.1 Correlation method

The output data from the bathymetric sonar are the (x, y, z) - coordinates for each beam's footprint against the bottom. The correlation sum used is

$$e^2 = \frac{1}{MN}\sum_{m=1}^{M}\sum_{n=1}^{N}\beta_{m,n}e_{m,n}^2 \,, \qquad (1)$$

where M is the number of pings and N is the number of beams in each ping. $\beta_{m,n}$ is a correction factor set to 1 in this paper. $e_{m,n}$ is the difference for each beam in depth between the map and the measured depth. Since the mean sea level often shifts during the day it is convenient at first to match only the bottom and the map profile against each other. This is done by first reducing the depth values by the mean depth value. The correlation is then done only in areas where the depth is approximately correct**.**

A typical result of a correlation is illustrated below**.** Here**,** the inverse of the correlation sum is plotted in the map position where the correlation is done.

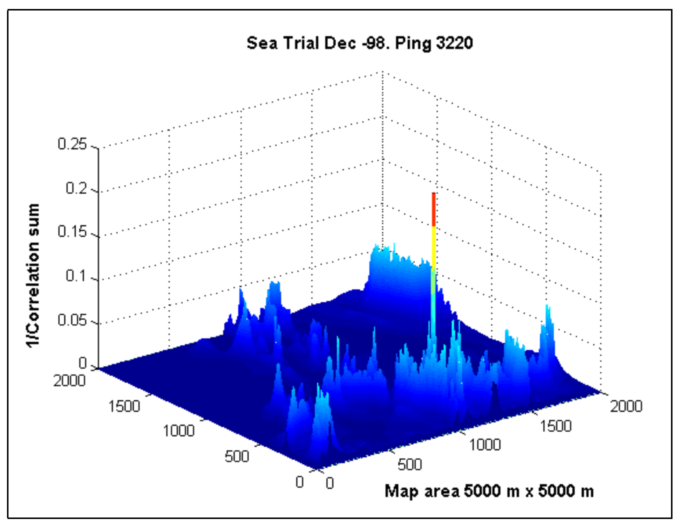

Figure 2.4. A typical correlation result with a single correlation peak showing the correct position. Ping 3220 in the sea trial.

The size of the navigation cell is 5000 m x 5000 m. As can be seen from the picture**,** a sharp peak indicates the correct position.

A different correlation measure is the median error

$$e = \frac{1}{MN}\sum_{m=1}^{M}\sum_{n=1}^{N}\beta_{m,n}\left|e_{m,n}\right| \qquad (2)$$

This correlation measurement is often more computationally efficient and in practice gives nearly the same performance as the correlation measurement described above. The performance of different correlation measurements in a similar context to this is evaluated in ref. [4].

The Figure 3.1 below illustrates the importance of the correlation length in sifting out the false positions from the true one.

A synthetic bottom profile was generated by a one-dimensional AR(1) process and a true position on the profile was chosen at random. A simulated sonar measurement of the bottom profile at that point was done with different correlation lengths, 20–340.

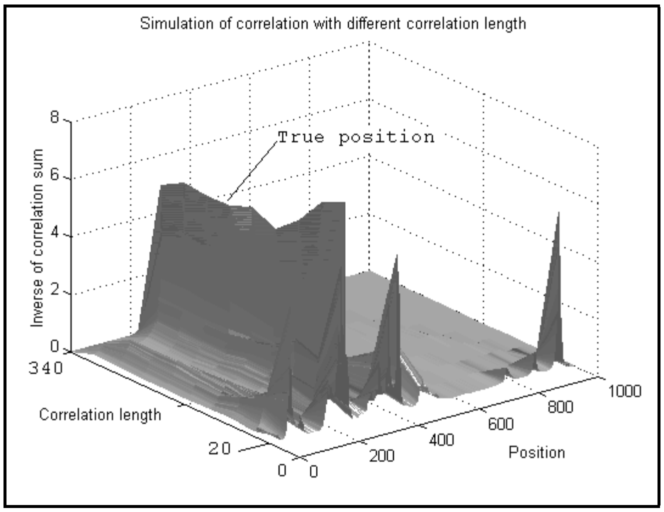

Figure 3.1. Correlation result versus correlation length and position showing some false locations for a short correlation length.

As can be seen from the Figure 3.1, there are several positions with high correlation when the correlation length is short. False positions are, however, rapidly dismissed with an increase in correlation length.

There are two causes for false positions:

- The bottom topography repeats itself.
- The measurement noise leads to the same correlation sum even if the bottom topography is different.

In both cases, an increase in correlation length will reduce the incidence of false positions. In the first case, it will be more unlikely that larger bottom areas have the same topography if the bottom is not completely flat.

3. Theoretical aspects

It is possible to reach high correlation of different locations due to similarities in the bottom structure and/or high measurement noise.

If we look at the one-dimensional case, N sonar beams, and assume that we have a sonar measurement of a bottom section, $\mathbf{s}_2 = \left[s_{2[1]},\ldots,s_{2[N]}\right]^T$, and we want to compare it with another part of the bottom profile, $\mathbf{s}_1 = \left[s_{1[1]},\ldots,s_{1[N]}\right]^T$, we can assume that the vectors $\mathbf{s}_1$ and $\mathbf{s}_2$ are Gaussian-distributed with a mean value of 0. Let the difference be $\mathbf{z} = \mathbf{s}_2 - \mathbf{s}_1$. The probability density function for the difference between that measurement and the map is then

$$f(\mathbf{z}) = \frac{1}{(2\pi)^{N/2}\sqrt{|\mathbf{C}|}} e^{-\frac{1}{2}\mathbf{z}^T\mathbf{C}^{-1}\mathbf{z}}, \tag{3}$$

where $\mathbf{C} = E\left\{\mathbf{z}\mathbf{z}^T\right\}$ is the covariance matrix for the vector $\mathbf{z}$.

If we assume that the bottom profile is generated by a stationary one dimensional AR(1) process we can make a LDL^* decomposition of the covariance matrix. The probability density function can then be expressed as a product

$$f(\mathbf{z}) \simeq f_1(y_1)\prod_{i=2}^{N} f_2(y_i), \tag{4}$$

where

$$f_1(y) = \frac{e^{\frac{-y^2}{2\sigma_1^2}}}{\sqrt{2\pi\sigma_1^2}} \quad (5) \qquad \text{and} \qquad f_2(y) = \frac{e^{\frac{-y^2}{2\sigma_2^2}}}{\sqrt{2\pi\sigma_2^2}} \quad (6)$$

The variances σ_1 and σ_2 depends on the distance between $\mathbf{s}_1$ and $\mathbf{s}_2$. The expression is exact for large distances and the error is small if $\mathbf{s}_1$ and $\mathbf{s}_2$ are close to each other. The probability that the difference between the measurement and the map is smaller than some value can be expressed as –

$$P(|z| \le \varepsilon) = \int_{-\varepsilon}^{\varepsilon} f_1(y)dy \cdot \left(\int_{-\varepsilon}^{\varepsilon} f_2(y)dy\right)^{N-1} \tag{7}$$

The probability that we will have the same correlation sum will therefore rapidly decrease as the correlation length increases.

This can also be seen as a kind of "pre-whitening" both the bottom profile and the measured profile and then calculating the probability that they are identical. The difference between the first and following factors is due to the end effect in the filter.

Above investigation was done for a one-dimensional AR(1) process; however, it is understood intuitively that the result will be similar for a two-dimensional AR(1) process.

With a different bottom topography, it is still possible to have false positions due to the measurement noise. If we let w denote the measurement noise we assume white Gaussian noise, with $E\{\mathbf{w}\}=0$. As before, we let $\mathbf{s_1}=\left[s_1[1],\ldots,s_1[N]\right]^T$ denote the one-dimensional map profile at the correct position.

The profile measured by the sonar is then $\mathbf{y}=\mathbf{s_1}+\mathbf{w}$ and the correlation sum –

$$T=(\mathbf{y}-\mathbf{s}_1)^T(\mathbf{y}-\mathbf{s_1})=\mathbf{w}^T\mathbf{w}=\sum_{i=1}^{N}w_i^2 \qquad (8)$$

which will be χ_N^2-distributed.

At another place we have a similar, but not identical, bottom profile, $\mathbf{s}_2=\mathbf{s}_1+\Delta\mathbf{s}$, where $\Delta\mathbf{s}$ is assumed to be Gaussian-distributed but correlated. The correlation sum for this section is –

$$T=(\mathbf{y}-\mathbf{s}_2)^T(\mathbf{y}-\mathbf{s}_2)=\mathbf{w}^T\mathbf{w}+\Delta\mathbf{s}^T\Delta\mathbf{s} \qquad (9)$$

The last term can be brought to a χ_N^2 distribution by first decorrelating the random variables Δs_i in the $\Delta\mathbf{s}$ vector by a modal decomposition of the covariance matrix, $C_s=E\{\Delta\mathbf{s}\Delta\mathbf{s}^T\}=V\Lambda V^T$. The correlation sum can therefore be written as –

$$T=\sum_{i=1}^{N}\alpha_i z_i^2 \text{, where } z_i \text{ is } N(0,1) \text{ and} \qquad (10)$$

$$\alpha_i=\sigma_{s,i}^2+\sigma_w^2 \qquad (11)$$

where σ_w is the noise variance and $\sigma_{s,i}^2=\lambda_{s,i}$ the eigenvalues of C_s (ref. [5, 6]).

We have also -

$$E\left\{\frac{T}{N}\right\}=\sigma_s^2+\sigma_w^2 \qquad (12)$$

$$Var\left\{\frac{T}{N}\right\}=\frac{2\|\mathrm{C}\|_F^2}{N^2}=\frac{2\sigma_w^2}{N}+\frac{4\sigma_s^2}{N^2}\sum_{i=1}^{N-1}(N-i)a^{2i} \qquad (13)$$

Where $\|C\|_F$ is the Frobenius norm of the covariance matrix and a the correlation coefficient for the bottom profile, see Figure 3.3.

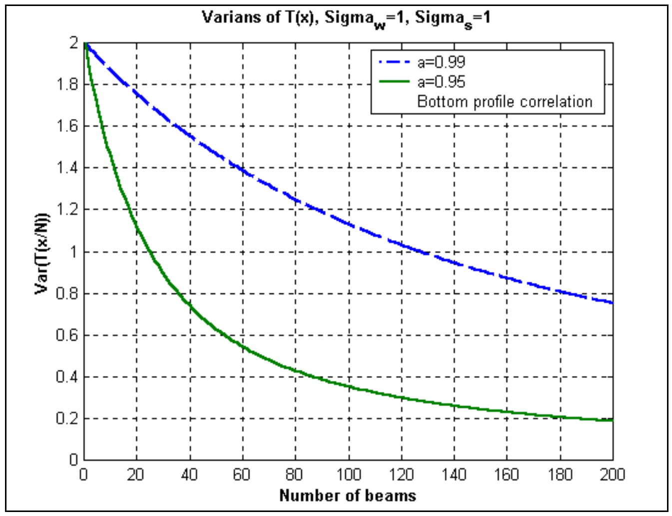

Figure 3.3. The variance of the correlation sum as a function of the number of beams, N.

The probability density function for T can be solved by using the principle of generating function. The characteristic function for a χ_1^2- distributed random variable is

$\phi_{\chi_1^2}=\dfrac{1}{\sqrt{1-2j\omega}}$ and the characteristic function for T will therefore be –

$$\phi_T(\omega)=\prod_{i=1}^{N}\frac{1}{\sqrt{1-2j\alpha_i\omega}} \qquad (14)$$

The inverse Fourier transform gives –

$$p_T(t)=\begin{cases}\displaystyle\int_{-\infty}^{\infty}\left(\prod_{i=1}^{N}\frac{1}{\sqrt{1-2j\alpha_i\omega}}\right)\cdot e^{-j\omega t}\cdot\frac{d\omega}{2\pi} & \text{för } t\geq 0\\ 0 & \text{för } t<0\end{cases}$$

(15)

Figures 3.3 and 3.4 below show the significance of the correlation length on the probability distributions for the correlation sum *T*.

Each of the Figures describes a scenario where we have two positions, one with a profile that differs little from the measured profile and one with a profile that differs much more from the measured profile. With a correlation length of 20, there is an large overlap between the distributions and we may misjudge the actual position.

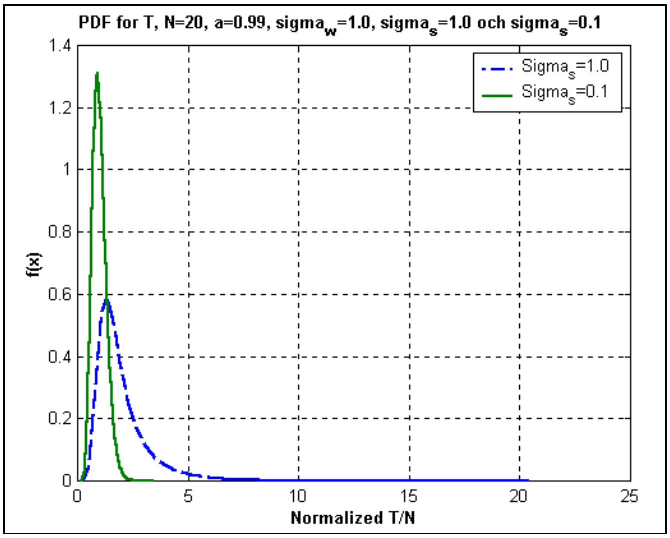

Figure 3.3. Probability density function for the correlation sum if N=20.

With a correlation length of 120, however, the distributions are better separated and the risk of wrong positioning is much smaller.

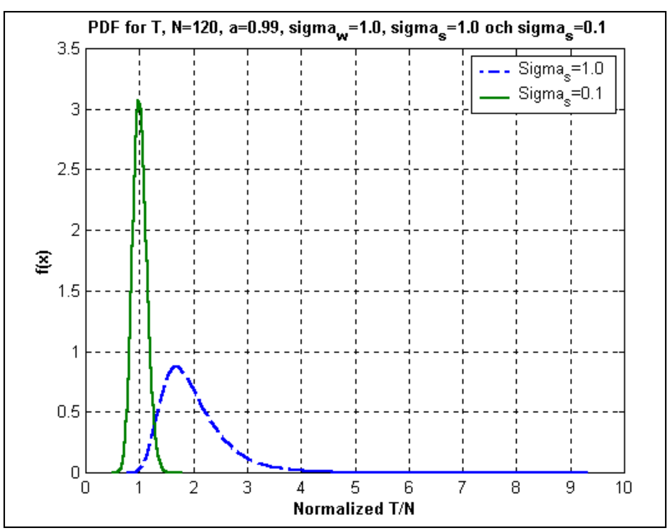

Figure 3.4. Probability density function for the correlation sum if N=120.

4. Simulation study

Many different methods can be used for determining the position from the underwater bottom map and a simulation study was therefore conducted to study the positioning error and its probability distribution for different positioning methods.

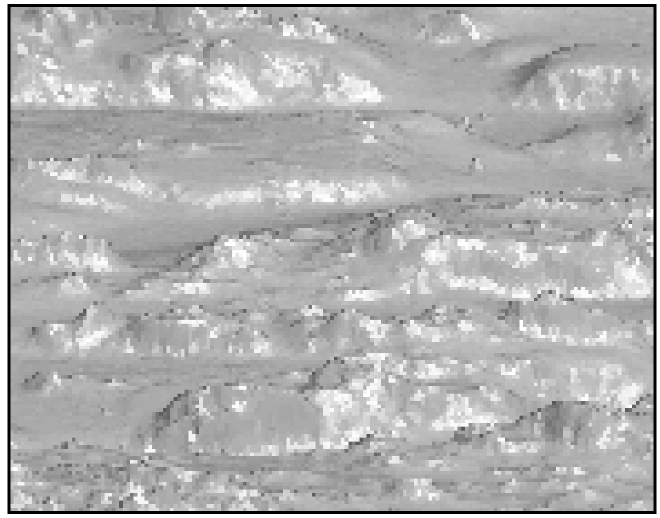

Figure 4.1. A typical area, approx. 2000 m x 2000 m, on the bottom map used in the simulation study. The vertical scale is 5 times enlarged.

Figure 4.1 above shows part of the bottom map used in the study. The map area was 5 000 m x 5 000 m and the depth varied between 25 m and 120 m.

The map was considered to be perfectly accurate in the horizontal directions. In the vertical direction, two different sizes of Gaussian random errors were considered, σ^2=0.5 m^2 and σ^2=1.0 m^2. The sea trials that were done later show that the larger error variance is more realistic due to the map's horizontal error.

The sonar used in the study was the Reson SeaBat 9001 and the same sonar was used in the sea trials. The SeaBat 9001 sonar has 60 beams with a beam width of 1.5 x 1.5º. The frequency is 455 kHz. The sonar is a Mills Cross design. The range resolution is 0.05 m. The measurement error and the error due to the ship's movement were included in the map error.

The beams were modeled as rays and no ray bending was included; in other words, there was no temperature gradient in the water.

The beam intersection with the map was calculated by interpolation individually for each beam. The map error was then added to the calculated depth.

Correlation according to equation (1) was then done against the whole map in steps of 1 m in the *x*- and *y*-directions horizontally. Different numbers of beam planes (pings) were used.

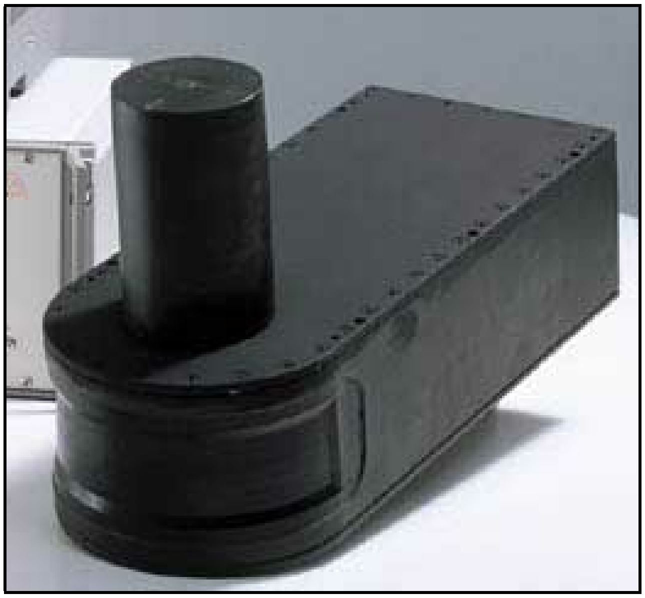

Figure 4.2. The SeaBat 9001 sonar used in both the simulation study and the sea trials.

Correlation with only one beam plane gives many possible locations. Simultaneous correlation with two beam planes considerably reduces the number of possible locations and usually three beam planes gave a unique position. Figure 4.3, next page, illustrates the sifting effect of the number of beam planes.

In order to study the positioning accuracy, a position was randomly chosen on the map and correlation was then done in a square area of 500 m x 500 m with the exact position in the middle. The following results were achieved when three beam planes were used in the correlation:

	σ^2=0.5 m^2	σ^2=1.0 m^2
No. of trials	19	21
Mean (m)	4.7	4.4
Sd (m)	2.3	3.0

Table 4.1. Mean and standard deviation (Sd) when three beam planes were used.

Correlation with four beam planes at the same time showed only minor improvements in the simulation study. However, in the evaluation of the sea trial, five beam planes were found to be more optimal.

The three-dimensional (3D) sonar was simulated as a sweep of ten beam planes (pings), each with ten beams.

Figures 4.4 and 4.5 below give the corresponding histogram.

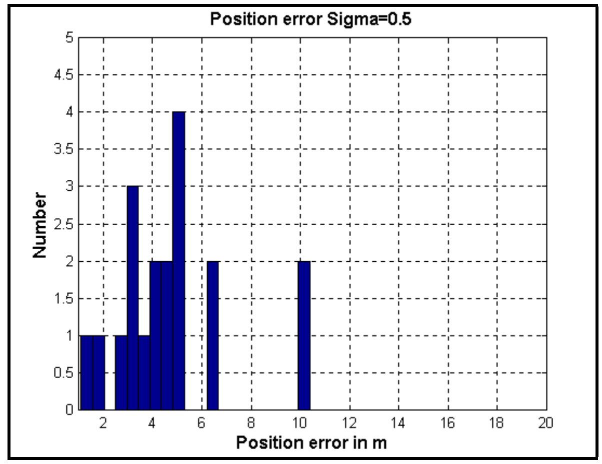

Figure 4.4. Histogram for the radial positioning error if σ^2=0.5 m^2.

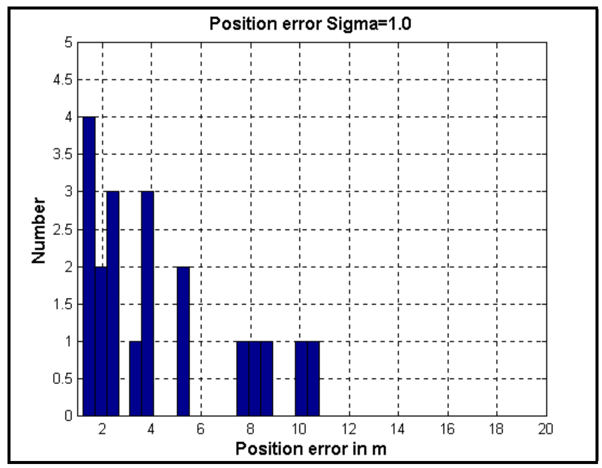

Figure 4.5. Histogram for the radial positioning error if σ^2=1.0 m^2.

The footprint against a flat bottom was as indicated in Figure 4.6.

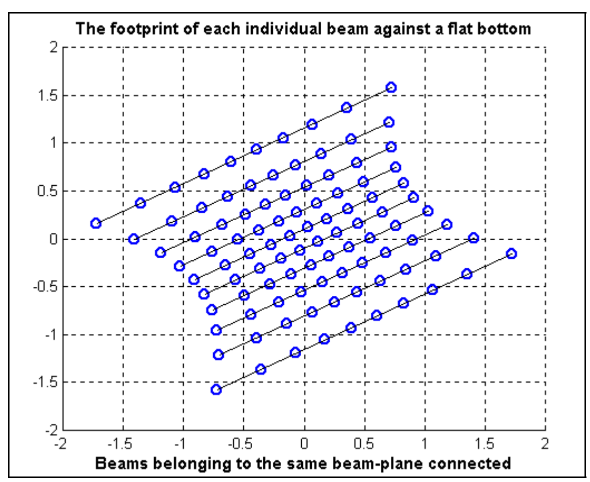

Figure 4.6. Footprint pattern for the individual beams in the model of the three-dimensional sonar.

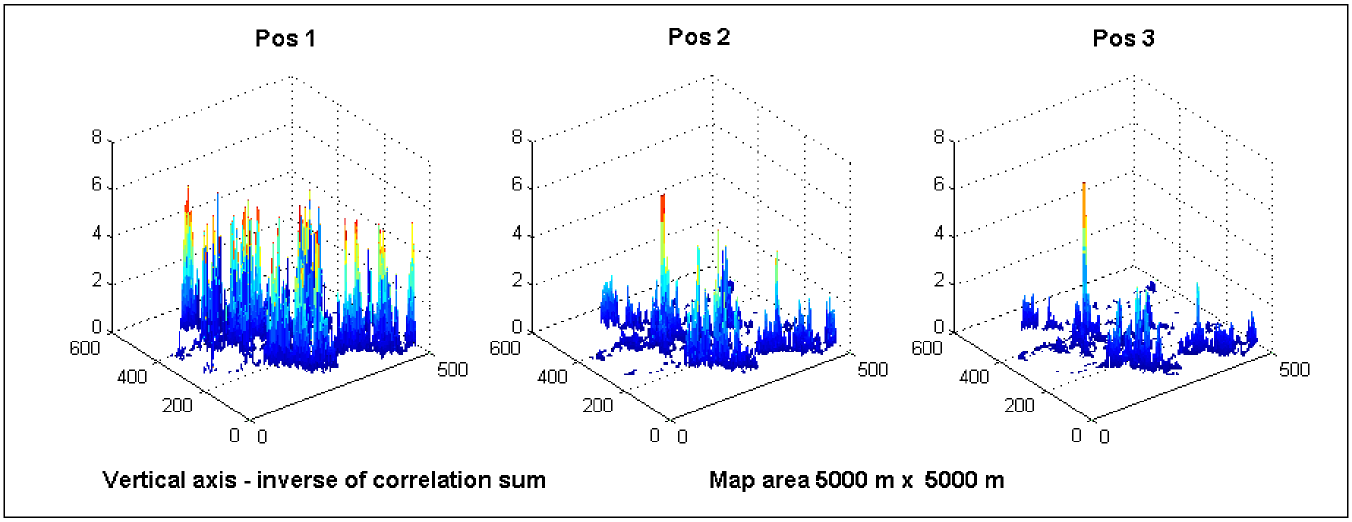

Figure 4.3. The sifting effect of using several beam planes. The graph on the left shows any possible locations after the first ping, and that in the middle shows locations after two pings**.** The graph on the right shows the remaining possible locations after three pings.

The simulation of the 3D sonar gave unique and excellent positioning results. A typical correlation result is illustrated in Figure 4.7.

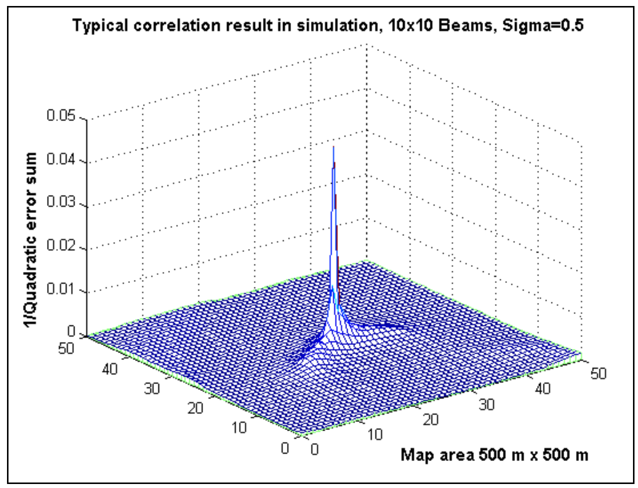

Figure 4.7. A typical correlation result for the three-dimensional sonar model.

Simulations were also done with different numbers of beams covering the same bottom area and it was found that even small numbers such as 5 x 5 beams give good results. The size of the area covered by the beams is more important than is the number of beams.

Using different numbers of beams corresponds with using different sampling distances and must of course be in agreement with the spatial frequency content of the bottom profile.

5. The sea trial

A sea trial was conducted in order to verify the simulation results. The SeaBat 9001 sonar was mounted below a small boat and the boat's position was measured by a DGPS receiver with 5 m accuracy. The boat's track was a figure of eight and the total distance was approx. 18 km. The distance traveled between the sonar pings was approx. 1.2 m. At approximately every 1000 pings**,** the horizontal position was afterwards determined by correlation with the bottom map. Correlation was only done if there was a height difference of at least 1 m in the correlation area.

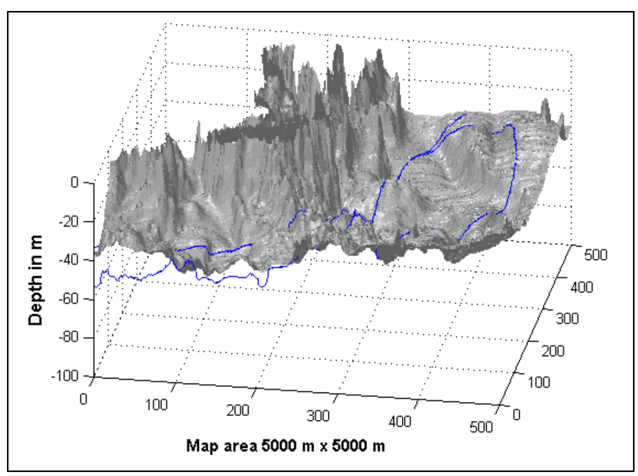

Figure 5.1. The bottom map of the area where the sea trial was conducted. The boat's track is indicated by the solid blue line.

The area where the sea trial was conducted was fairly flat. Figure 5.1 shows the bottom map with the boat's track indicated in blue. The vertical scale in the Figure has been enlarged approximately 24 times.

The results of positioning at the different places are very similar and all positions compared with the DGPS positions have small radial positioning errors.

Figure 5.2 shows the bottom at the location for ping 2220. As can be seen, the bottom is fairly smooth. The bottom at the other locations shows similar characteristics. The depth at that ping location was approx. 45 m.

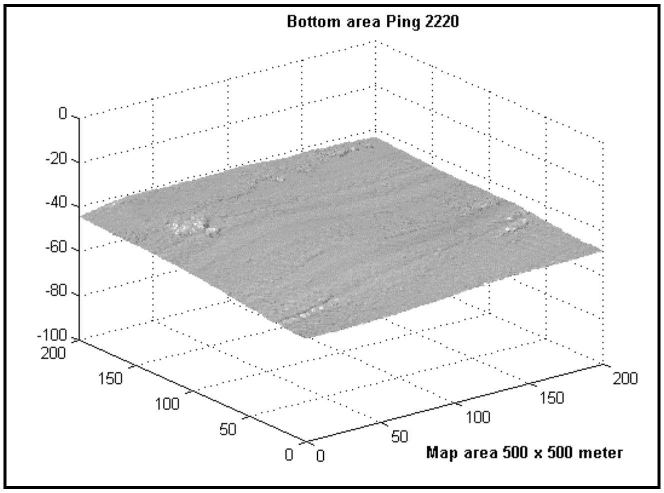

Figure 5.2. Bottom at ping 2220. Vertical axis in meter.

The inverse of the normalized correlation error at ping 2220 is shown in Figure 5.3. The correlation error is calculated in steps of 1 m on the underwater map. The grid size of the map was 2.5 m and interpolation of the depths on the map was used.

In the correlation, it was found that using five beam planes gave significantly better results than did using only three beam planes, as in the simulations. Correlation with ten beam planes gave almost no improvement.

The relative position of the beam planes to each other was calculated using the DGPS and it can be anticipated that the benefits of using more beam planes will be neutralized by the error in relative positions of the beam planes.

Compared with the DGPS position at ping 2220, the highest correlation peak had an error of 3.6 m in the *x*-direction and 2.4 m in the *y*-direction. However, despite the small positioning error, it can be seen that there is a secondary peak close to the correct position. Figure 5.4 shows a close-up of the two points.

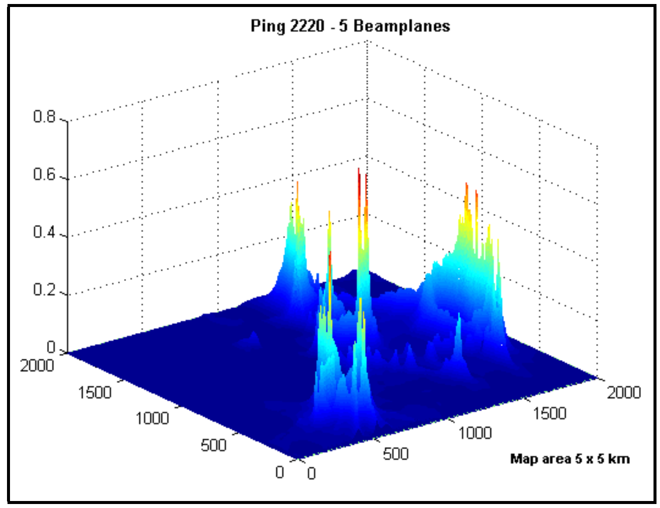

Figure 5.3. Correlation results at ping 2220.

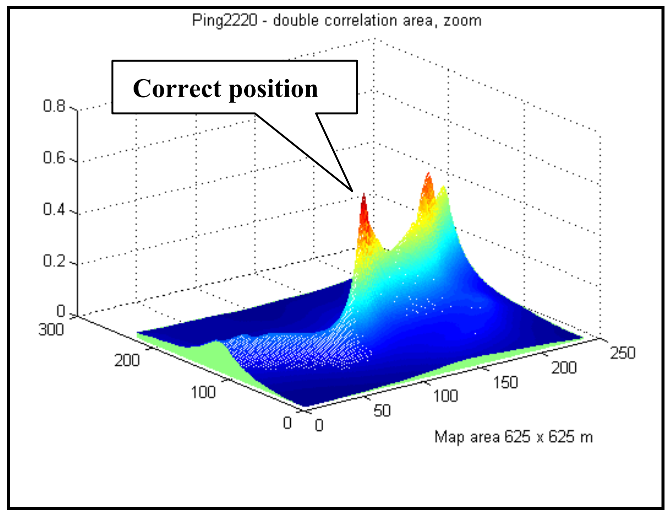

Figure 5.4. Zoom of the correlation peaks at ping 2220.

From the theoretical aspects in Section 3, it is clear that enlarging the correlation area will largely reduce the problem of secondary peaks. And as can be seen from Figure 5.5, this is indeed the case. The correlation area was increased from approx. 45 m x 90 m to 90 m x 90 m.

As with the beam planes, it can be expected that the increase in performance will be hampered by the increase in relative error between the beam planes when the correlation area increases.

The sea trial was done with a DGPS receiver with a nominal position accuracy of 5 m and it could be expected that the matching performance would increase, especially in flat areas, if the relative positioning error between the beam planes was kept low.

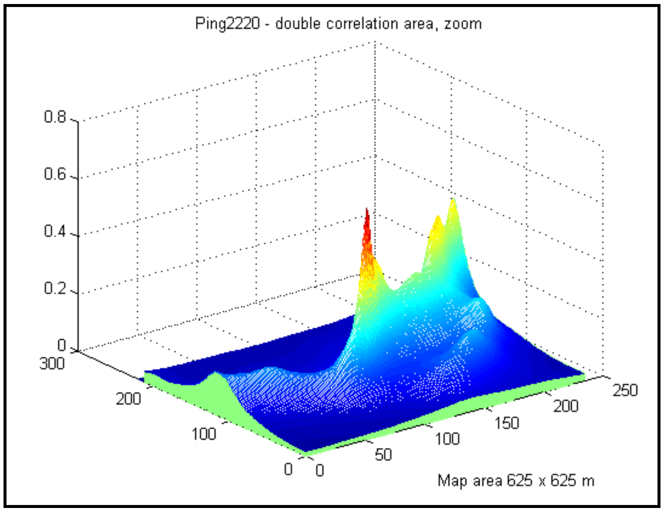

Figure 5.5. Zoom of the correlation peaks at ping 2220 when the size of the correlation area was doubled.

A very preliminary sea trial was therefore done with the 3D sonar EchoScope (OmniTech, Bergen, Norway).

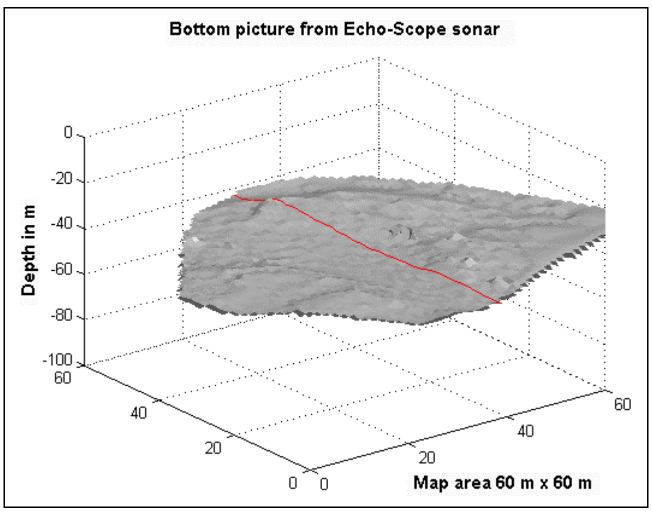

Figure 5.6. A typical bottom map of the three-dimensional sonar EchoScope from OmniTech.

The 3D sonar captures the bottom topography in only one ping and it is anticipated that the relative positioning error between the individual beams will be very small and therefore give the full benefit of increasing the correlation area. Figure 5.6 gives a typical bottom map captured by the 3D sonar. The correlation area is approx. 40 m x 60 m.

6. Conclusions

It has been shown that it is possible for an AUV to accurately determine its position in a previously mapped area by measuring the bottom topography with a few pings from a conventional bathymetric sonar and then correlating the measurement against the map.

If a unique position is not obtained at first, an increase of the correlation area will often resolve the problem of competing correlation peaks.

7. References

[1] Oddjörn Bergem: Bathymetric Navigation of Autonomous Underwater Vehicles using a Multibeam sonar and a Kalman Filter with Relative Measurement Covariance Matrices. Doctoral thesis, 1993. Institutt for Informatik, AVH. University of Trondheim, Trondheim, Norway.

[2] Niclas Bergman: Recursive Bayesian Estimation: Navigation and Tracking Applications. Ph.D. thesis 579, Linköping University, Division of Automatic Control, Linköping, Sweden, 1999.

[3] Lennart Kullander: Development of a Terrain Navigation System for AUVs. Proceedings of the International Symposium on Unmanned Untethered Submersible Technology, pp. 494-501, Durham, NH, USA, June 1989.

[4] Carl-Johan Andersson: Navigation System for an Autonomous Underwater Vehicle. Masters thesis on Automatic Control, Royal Institute of Technology, Stockholm, Sweden, 2000.

[5] Steven M. Kay: Fundamentals of Statistical Signal Processing, Detection Theory, Prentice Hall, 1993.

[6] Norman L, Samuel Kotz, N. Balakrishnan: Continuous Univariate Distributions, John Wiley & Sons, 1994.

[7] Ingemar Nygren: Terrängnavigering för undervattensfarkoster. FOA–R—00-01777-313—SE, December 2000. (In Swedish.)